

Published in final edited form as:

*J Mol Cell Cardiol.* 2011 November ; 51(5): 632–639. doi:10.1016/j.yjmcc.2011.05.007.

## Dynamic modulation of Ca<sup>2+</sup> sparks by mitochondrial oscillations in isolated guinea pig cardiomyocytes under oxidative stress

Lufang Zhou, Miguel A Aon, Ting Liu, and Brian O'Rourke

Department of Medicine, Division of Cardiology, The Johns Hopkins University School of Medicine, Baltimore, MD 21205

### Abstract

Local control of Ca<sup>2+</sup>-induced Ca<sup>2+</sup> release (CICR) depends on the spatial organization of L-type Ca<sup>2+</sup> channels and ryanodine receptors (RyR) in the dyad. Analogously, Ca<sup>2+</sup> uptake by mitochondria is facilitated by their close proximity to the Ca<sup>2+</sup> release sites, a process required for stimulating oxidative phosphorylation during changes in work. Mitochondrial feedback on CICR is less well understood. Since mitochondria are a primary source of reactive oxygen species (ROS), they could potentially influence the cytosolic redox state, in turn altering RyR open probability. We have shown that self-sustained oscillations in mitochondrial inner membrane potential ( $\Delta\Psi_m$ ), NADH, ROS, and reduced glutathione (GSH) can be triggered by a laser flash in cardiomyocytes. Here, we employ this method to directly examine how acute changes in energy state dynamically influence resting Ca<sup>2+</sup> spark occurrence and properties. Two-photon laser scanning microscopy was used to monitor cytosolic Ca<sup>2+</sup> (or ROS),  $\Delta\Psi_m$ , and NADH (or GSH) simultaneously in isolated guinea pig cardiomyocytes. Resting Ca<sup>2+</sup> spark frequency increased with each  $\Delta\Psi_m$  depolarization and decreased with  $\Delta\Psi_m$  repolarization without affecting Ca<sup>2+</sup> spark amplitude or time-to-peak. Stabilization of mitochondrial energetics by pretreatment with the superoxide scavenger TMPyP, or by acute addition of 4'-chlorodiazepam, a mitochondrial benzodiazepine receptor antagonist that blocks the inner membrane anion channel, prevented or reversed, respectively, the increased spark frequency. Cyclosporine A did not block the  $\Delta\Psi_m$  oscillations or prevent Ca<sup>2+</sup> spark modulation by  $\Delta\Psi_m$ . The results support the hypothesis that mitochondria exert an influential role on the redox environment of the Ca<sup>2+</sup> handling subsystem, with mechanistic implications for the pathophysiology of cardiac disease.

### Keywords

reactive oxygen species; calcium sparks; bioenergetics; mitochondrial inner membrane; oxidative; phosphorylation; ryanodine receptor; antioxidants; redox biology

© 2011 Elsevier Ltd. All rights reserved.

Correspondence to: Brian O'Rourke, Ph.D., Division of Cardiology, The Johns Hopkins University School of Medicine, 720 Rutland Ave, Ross Bldg 1060, Baltimore, MD 21025, bor@jhmi.edu, Phone: 410-614-0034, Fax: 410-502-5055.

**Publisher's Disclaimer:** This is a PDF file of an unedited manuscript that has been accepted for publication. As a service to our customers we are providing this early version of the manuscript. The manuscript will undergo copyediting, typesetting, and review of the resulting proof before it is published in its final citable form. Please note that during the production process errors may be discovered which could affect the content, and all legal disclaimers that apply to the journal pertain.

**Disclosures:** None

## Introduction

Structural and functional evidence suggests that a mitochondrial microdomain exists near the dyad in cardiac myocytes (reviewed in [1]). Electron micrographs show that t-tubules and  $\text{Ca}^{2+}$  release junctions are typically sandwiched between mitochondria at the z-line, with the mesh-like corbular SR (containing the SR  $\text{Ca}^{2+}$  pumps) wrapping around the mitochondria [2]. The large spike in junctional  $\text{Ca}^{2+}$  (50–100  $\mu\text{M}$ ) during  $\text{Ca}^{2+}$ -induced  $\text{Ca}^{2+}$  release (CICR) and the close proximity of mitochondria to the  $\text{Ca}^{2+}$  release sites (40–300 nm) are thought to promote rapid mitochondrial  $\text{Ca}^{2+}$  uptake, leading to matrix  $\text{Ca}^{2+}$  accumulation and the consequent stimulation of oxidative phosphorylation. This mechanism is essential for matching energy supply with demand [2, 3].

In addition to the feedforward effect of  $\text{Ca}^{2+}$  on bioenergetics [4], feedback of mitochondrial function on  $\text{Ca}^{2+}$  cycling is also expected. Ion pumps in the sarcolemma ( $\text{Na}^+/\text{K}^+$  ATPase,  $\text{Ca}^{2+}$  ATPase) and the  $\text{Ca}^{2+}$  ATPase of the sarcoplasmic reticulum (SERCA2a) depend on the free energy of ATP hydrolysis [5], and the L-type  $\text{Ca}^{2+}$  channel [6, 7], the  $\text{Na}^+/\text{Ca}^{2+}$  exchanger [8] and the RyR [9] are also modulated by ATP, ADP and  $\text{Mg}^{2+}$ . In general, mitochondrial  $\Delta\Psi_m$  depolarization and decreased ATP production tend to suppress the activity of these  $\text{Ca}^{2+}$  transport proteins.

Another important functional role of mitochondria is that they are both a source and a target of ROS [10–12]. Under normal conditions, up to 1% of the electrons flowing to  $\text{O}_2$  through the electron transport chain may be diverted to form superoxide ( $\text{O}_2^-$ ), which is subsequently dismutated to hydrogen peroxide ( $\text{H}_2\text{O}_2$ ) by superoxide dismutase and then converted to  $\text{H}_2\text{O}$  by glutathione peroxidase and/or catalase [13]. Under normal conditions, there is a balance between ROS formation and antioxidant activity; however, under pathological conditions, oxidative stress can be initiated by either an increase in ROS production or by depletion of the antioxidant pool [14, 15], leading to collapse of the mitochondrial membrane potential, an effect that is amplified by the mechanism of mitochondrial ROS-induced ROS release (RIRR) [16]. Studies from our laboratory have demonstrated that local oxidative stress produced by a laser flash in a few mitochondria can trigger self-sustaining cell-wide oscillations in  $\Delta\Psi_m$  and the redox states of the pyrimidine nucleotide [15] and glutathione pools [16] in cardiomyocytes.

The dramatic changes in  $\Delta\Psi_m$  and intracellular redox state are likely to have important effects on CICR, especially considering that the RyR has been described as a redox sensor with a well-defined midpoint owing to the presence of highly reactive clusters of cysteines [17]. Oxidation of these reactive thiols markedly increases RyR open probability, whereas reduction suppresses channel activity. Here, we utilize the stereotypical pattern of triggered oscillations in mitochondrial energy state to determine if RyR channels are dynamically regulated through changes in cytoplasmic redox potential governed by mitochondria in the proximity of the  $\text{Ca}^{2+}$  release sites. We show, for the first time, that the resting  $\text{Ca}^{2+}$  spark frequency is dynamically modulated by the mitochondrial energetic and redox status. We also demonstrate that the oscillatory mechanism involves benzodiazepine-sensitive mitochondrial ion channels but not the permeability transition pore (PTP).

## 2. Material and Methods

All protocols involving animals conformed to the *Guide for the Care and Use of Laboratory Animals* published by the US National Institutes of Health (NIH Publication No. 85–23, revised 1996) and were approved by the Johns Hopkins Animal Care and Use Committee.

## 2.1 Cardiomyocyte isolation and loading of fluorescent probes

All experiments were carried out at 37 °C on freshly isolated adult guinea pig ventricular myocytes prepared by enzymatic dispersion as previously described.[18] Briefly, animals of either sex were anaesthetized with sodium pentobarbital (30 mg/kg I.P.). Following thoracotomy, hearts were quickly excised, mounted on a Langendorff apparatus, and perfused with collagenase-containing solution at 37°C. After isolation, cells were stored in a high K<sup>+</sup> solution (in mmol/L: 120 Glutamate, 25 KCl, 1 MgCl<sub>2</sub>, 10 HEPES, 1 EGTA, and pH 7.5 with KOH) temporarily. The cationic potentiometric fluorescent dye tetramethyl rhodamine methyl ester (TMRM) was used to monitor changes in  $\Delta\Psi_m$ . ROS production was monitored with MitoSOX (Invitrogen), a superoxide-sensitive fluorescent indicator. The localizations of TMRM and MitoSOX within the mitochondria were shown in the supplemental materials (figure S1). To image the distribution of  $\Delta\Psi_m$  (or ROS) and Ca<sup>2+</sup> simultaneously, 100 nM TMRM (or 2  $\mu$ mol/L MitoSOX) and 4  $\mu$ mol/L fluo-4 AM were added to the external solution and allowed to equilibrate for at least 25 min at 37°C. After loading, the cells were resuspended in the experimental solution for 20 min to permit de-esterification of the dye before recording images. To monitor the intracellular reduced glutathione (GSH) and  $\Delta\Psi_m$  simultaneously, cells were loaded with 50  $\mu$ mol/L monochlorobimane (MCB) and TMRM as described previously [14].

## 2.2 Image Acquisition and Analysis

The dish containing the cardiomyocytes was equilibrated at 37°C with unrestricted access to atmospheric oxygen on the stage of a Nikon E600FN upright microscope. Images were recorded using a two-photon laser scanning microscope (Bio-Rad MRC-1024MP) with excitation at 760 nm (Tsunami Ti:Sa laser, Spectra Physics) as described previously [15]. Because of the overlap in the cross-sections for two-photon excitation of the three fluorophores of interest (NADH or GSB, Fluo-4, and TMRM or MitoSOX), this wavelength permitted recording of redox, Ca<sub>2+</sub>, and  $\Delta\Psi_m$  or ROS simultaneously. A three channel photomultiplier detector assembly with appropriate dichroic mirrors and bandpass filters was used to separate the fluorescence emissions of the blue (<500nm for NADH or 480 nm for GSB), green (500–550nm; Fluo-4) and red (580–630nm; TMRM or MitoSOX) indicators with no crossover between the signals. For fast time resolution of Ca<sub>2+</sub> sparks, the line-scan mode of the two-photon microscope was used. 512 × 512 pixel line-scan images (2msec/line) were acquired every 3.7 sec and the three emissions were collected and stored simultaneously as 8-bit/channel grayscale images. The frequency of false event detection was determined by measuring Ca<sub>2+</sub> spark frequency in the absence of an SR Ca<sub>2+</sub> load (i.e., after 3–5 minutes of 1Hz pacing and blocking SR Ca<sub>2+</sub> uptake with 1  $\mu$ mol/L thapsigargin). The frequency of Ca<sub>2+</sub> sparks with a fully loaded SR was also measured after pacing during isoproterenol exposure. The average Ca<sub>2+</sub> spark frequency was 0.28 with the SR depleted (false event rate) and 27.5 sparks/100 $\mu$ m/s for a highly loaded SR (figure S2). Mitochondrial depolarization was induced either by applying a localized laser flash (e.g. the result shown in Figure 1) to a small (~64 micron<sup>3</sup>) region of the cell volume [15] or by repeated line scanning at the selected mitochondrial row (e.g., Figure 2). Images were analyzed offline using ImageJ software (Wayne Rasband, National Institutes of Health) and Ca<sup>2+</sup> sparks were analyzed using a recently developed ImageJ plug-in [19].

Wide-field fluorescence images of TMRM (shown in Figure 3B) were acquired using a high-sensitivity CCD camera (Cascade II; Photometrics).

## 2.3 Experimental Protocol

In the present study, four groups of non-beating cells were studied under different experimental conditions in order to investigate the effects of mitochondrial energy state on resting Ca<sup>2+</sup> spark frequency. **CON group:** image recording was started immediately after

cell loading in modified Tyrode's solution containing (in mmol/L) 140 NaCl, 5 KCl, 1 MgCl<sub>2</sub>, 10 HEPES, 1 CaCl<sub>2</sub>, pH 7.5 (adjusted with NaOH), supplemented with 10 mmol/L glucose; **TMPyP group**: 200 μmol/L Mn(III)tetrakis(1-methyl-4-pyridil) porphyrin pentachloride (TMPyP) was added to the Tyrode's solution and the cell suspension was pre-incubated for 2h with gentle shaking before image recording; **4'Cl-DZP group**: experiments were started with normal Tyrode's, and after mitochondrial oscillations were observed, 20 μmol/L 4'-chlorodiazepam (4'Cl-DZP) was added to the perfusion chamber before resuming the image acquisition; **CsA group**: experiments were started with normal Tyrode's, and after mitochondrial oscillations were detected, 1 μmol/L cyclosporin A (CsA) was added to the perfusion chamber, and image acquisition was continued.

## 2.4 SR Ca<sup>2+</sup> load measurements

Myocytes were whole-cell patch-clamped at 37°C as previously described [3]. Briefly, cells were placed in a heated chamber on the stage of an inverted fluorescence microscope (Eclipse TS100 inverted microscopes, Nikon, Inc.) and superfused with solution containing (in mmol/L) 140 NaCl, 110 CsCl, 1 MgCl<sub>2</sub>, 10 HEPES, 10 Glucose, and 2 CaCl<sub>2</sub>, pH 7.4. Internal solution contains (in mmol/L) 138 potassium glutamate, 10 Na-HEPES, and 5 Mg-ATP, pH 7.2. Borosilicate glass pipettes of 2–3 MΩ tip resistance were used for whole-cell recording with an Axopatch 1D amplifier coupled to a Digidata 1200A personal computer interface (Axon Instruments, Foster City, CA) using custom-written software. After whole-cell configuration was established, 10 mmol/L caffeine was introduced with a custom-built heated rapid-switching device as described previously and NCX current evoked by caffeine-induced SR Ca<sup>2+</sup> release was measured following a 3 minutes train. SR Ca<sup>2+</sup> contents were calculated by integrating the area under the curve (AUC) of NCX current. Then the cell was exposed to a UV light (exposure time: 1 second), which depolarized the mitochondrial network in ~3–5 minutes (Figure 3B). The NCX current was measured again and compared with that obtained before mitochondrial depolarization.

## 2.5 Materials

TMRM, MCB and Fluo-4-AM were purchased from Invitrogen Corp (Carlsbad, CA). 4'Cl-DZP and CsA were obtained from Sigma-Aldrich (St. Louis, MO). TMPyP was purchased from Calbiochem (San Diego, CA). All other reagents were from Sigma. Stock solutions of these reagents were prepared in DMSO and concentrated enough to avoid exceeding 0.1% DMSO (v/v) in the final solution.

## 2.6 Statistics

Comparisons were performed using paired or unpaired 2-tailed Student's t test. Data were considered significantly different at  $p < 0.05$ . Results are presented as mean ± SEM.

## 3. Results

### 3.1 Oscillations in mitochondrial energetics drive cyclical changes in resting Ca<sup>2+</sup> spark frequency

In order to analyze the dependence of resting Ca<sup>2+</sup> spark frequency on the mitochondrial energy state, experiments were performed on isolated guinea pig cardiomyocytes in the absence of electrical stimulation. As expected from our previous work, a localized laser flash in freshly isolated cardiomyocytes triggered cell-wide oscillations in  $\Delta\Psi_m$  and NADH, which was confirmed by monitoring full field images (data not shown) at the onset of the experiment. The imaging system was then switched to line-scan mode across the longitudinal axis of the cell and  $\Delta\Psi_m$ , Ca<sup>2+</sup>, and NADH signals were collected simultaneously. Analysis of the Fluo-4 images revealed that resting Ca<sup>2+</sup> spark frequency

increased with each depolarization of  $\Delta\Psi_m$  and decreased upon  $\Delta\Psi_m$  repolarization over several cycles of  $\Delta\Psi_m$  oscillation (Figure 1A). A representative contour plot of  $\text{Ca}^{2+}$  sparks during mitochondrial polarization or depolarization is shown in figure 1B. Average  $\text{Ca}^{2+}$  spark frequency was  $8.2\pm 4.6$  (sparks/100 $\mu\text{m/s}$ ) when  $\Delta\Psi_m$  was polarized versus  $21.4\pm 3.4$  (sparks/100 $\mu\text{m/s}$ ) when  $\Delta\Psi_m$  was depolarized, showing a 2.5 fold increase in  $\text{Ca}^{2+}$  spark frequency (Figure 1C). Whole cell diastolic  $\text{Ca}^{2+}$  did not change during mitochondrial membrane potential oscillation, as revealed by the average Fluo-4 fluorescence intensity (figure 1A, green line).

Repeated line scanning in the absence of a laser flash was also shown to trigger  $\Delta\Psi_m$  and NADH oscillations in some cells that were under highly stressed conditions (Figure 2A). In this case,  $\text{Ca}^{2+}$  spark frequency oscillated between  $4.1\pm 0.8$  and  $12.2\pm 1.1$  sparks/100 $\mu\text{m/s}$  ( $p<0.05$ ) when mitochondria were polarized and depolarized, respectively (Figure 2B). However, no significant changes were detected in other properties of the  $\text{Ca}^{2+}$  sparks such as amplitude, full width at half-max (FWHM), and time-to-peak (Figures 2C-2E).

To determine whether SR  $\text{Ca}^{2+}$  content is involved in the regulation of  $\text{Ca}^{2+}$  spark frequency, the SR  $\text{Ca}^{2+}$  content before and after mitochondrial depolarization were measured, respectively. For the example presented in figure 3, we observed only a modest increase in the NCX current (from 378 to 392 pA), reflecting a minor, statistically insignificant, change in SR  $\text{Ca}^{2+}$  content (in  $\mu\text{mol}$ ,  $33.0 + 5.0$  vs  $37.7 + 6.5$ ) immediately after mitochondria depolarization (Figure 3B). Small spikelike inward currents were also observed during the caffeine exposure; these were due to the opening of caffeine-sensitive channels of unknown identity in the guinea-pig sarcolemma which were independent of SR  $\text{Ca}^{2+}$  load (still present after thapsigargin treatment). They were excluded from the NCX integral analysis (supplemental materials, figure S5). There were no apparent changes in cellular morphology during the experiments.

### 3.2 Effects of ROS scavenging or mitochondrial ion channel inhibitors on resting $\text{Ca}^{2+}$ spark frequency

As we have previously proposed [15, 16], the mechanism of the ROS-dependent mitochondrial oscillator involves the activation of a benzodiazepine-sensitive inner membrane anion channel (IMAC) whose opening is triggered by mitochondrial  $\text{O}_2^{\cdot-}$  production. To demonstrate the common mechanistic basis of the modulation of  $\text{Ca}^{2+}$  sparks in the present work, we employed the  $\text{O}_2^{\cdot-}$  sensor MitoSOX, which preferentially localizes to mitochondria (supplemental materials, figure S1), the superoxide dismutase mimetic TMPyP, and the peripheral benzodiazepine receptor ligand 4'-chlorodiazepam (4'-Cl-DZP). During mitochondrial oscillation induced by oxidative stress, MitoSOX fluorescence increased in a stepwise manner in association with each oxidation of the NADH pool (Figure 4A), as expected because the oxidized product is not readily reduced in the cell. The increased rate of  $\text{O}_2^{\cdot-}$  production correlated with each cycle of oxidation, as indicated by plotting the first derivative of the raw MitoSOX fluorescence signal along with the NADH signal (Figure 4A). Accompanying mitochondrial oscillations, intracellular GSH concentration changes cyclically, with GSH depleted during the depolarization phase (Figure 4B). The TMPyP treatment decreased the overall rate of  $\text{O}_2^{\cdot-}$  production and prevented mitochondrial oscillation (Figure 4C), in accordance with its ability to keep ROS levels in the mitochondrial network below the threshold for mitochondrial criticality.[20] Again,  $\text{Ca}^{2+}$  spark frequency increased when mitochondria were depolarized (NADH oxidized) and this increase was prevented by pretreatment with 200  $\mu\text{mol/L}$  TMPyP for 2 hours (Figure 4D).

The mitochondrial benzodiazepine receptor ligand 4'-Cl-DZP inhibits IMAC [21] and prevents or reverses mitochondrial oscillation [15, 22]. In depolarized cells displaying

enhanced  $\text{Ca}^{2+}$  spark activity, the acute application of 4'Cl-DZP (20  $\mu\text{mol/L}$ ) rapidly recovered the NADH pool and stabilized  $\Delta\Psi_m$ , and  $\text{Ca}^{2+}$  spark frequency decreased concomitantly (Figure 5A and 6). The average  $\text{Ca}^{2+}$  spark frequency significantly decreased after 4'Cl-DZP from  $22.5 \pm 1.2$  to  $11.8 \pm 0.8$  sparks/100 $\mu\text{m/s}$  (Figure 5B).

Acute addition of the mitochondrial permeability transition pore (mPTP) blocker cyclosporine A (CsA) did not eliminate the  $\Delta\Psi_m$  oscillations (Figure 6A), nor did it prevent the modulation of the  $\text{Ca}^{2+}$  spark frequency by  $\Delta\Psi_m$ . However, in the presence of CsA (1  $\mu\text{mol/L}$ ), the peak  $\text{Ca}^{2+}$  spark frequency during  $\Delta\Psi_m$  depolarization ( $19.7 \pm 3.8$  sparks/100 $\mu\text{m/s}$ ) was less than in the absence of CsA in the same cell ( $35.2 \pm 2.1$  sparks/100 $\mu\text{m/s}$ ; Figure 6B). We also observed reduced  $\text{Ca}^{2+}$  spark frequency in non-oscillating myocytes upon high concentration (10 mmol/L) CsA treatment (supplemental materials, figure S2). 4'Cl-DZP (20  $\mu\text{mol/L}$ ) applied at the end of the experiment restored and stabilized  $\Delta\Psi_m$  and decreased resting  $\text{Ca}^{2+}$  sparks to control levels (Figures 5A and 6B).

#### 4. Discussion

The central finding of the present study is that the  $\text{Ca}^{2+}$  spark frequency in quiescent, non-beating cardiomyocytes is dynamically modulated by the mitochondrial energy state. During cell-wide oscillations of  $\Delta\Psi_m$ , mitochondrial depolarization was correlated with increased  $\text{Ca}^{2+}$  spark frequency, while repolarization suppressed  $\text{Ca}^{2+}$  spark frequency. The cyclical enhancement of  $\text{Ca}^{2+}$  spark frequency corresponded to the phase of high superoxide production by the mitochondrial electron transport chain, NADH oxidation, and depletion of the intracellular glutathione pool, consistent with our model of the ROS-dependent mitochondrial oscillator described previously in theoretical [16] and experimental [15] studies. The common mechanistic link between  $\Delta\Psi_m$  oscillations and  $\text{Ca}^{2+}$  sparks was demonstrated by concomitant suppression of mitochondrial oscillations and  $\text{Ca}^{2+}$  spark changes with the IMAC inhibitor 4'Cl-DZP, or by pretreatment of the cardiomyocytes with the superoxide scavenger TMPyP.

Over the past two decades, through ryanodine binding studies, SR  $\text{Ca}^{2+}$  release assays, and RyR channel reconstitution, it has been established that oxidation of critical sulfhydryl groups on the RyR increases the open probability of the channel, while thiol reducing agents have the opposite effect [23–27]. Moreover, it has been demonstrated the RyR is a redox sensor with a well-defined midpoint potential with respect to the glutathione redox state (GSH:GSSG) [17], the largest capacity antioxidant system of the cell. This sensitivity to the thiol state has been attributed to ~20–40 hyperreactive cysteines present on each monomer of the tetrameric RyR channel assembly [24, 28]. While a direct link between cysteine oxidation and RyR activity is undeniable, it has not been well established how this mechanism might come into play in intact cells or muscles. Several recent studies have examined the influence of mitochondrial function on  $\text{Ca}^{2+}$  sparks. For example, Isaeva et al [29] reported an increase in  $\text{Ca}^{2+}$  spark activity in skinned skeletal muscle fibers that correlated with oxidation of the mitochondrial NADH pool, but not SR  $\text{Ca}^{2+}$  content, and could be suppressed by treatment with ROS scavengers or mimicked by  $\text{H}_2\text{O}_2$  treatment. The onset of enhanced spark activity depended on the muscle type, with mitochondria-rich slow muscles having the longest delay. Mitochondrial ROS production has also been implicated in  $\text{Ca}^{2+}$  spark activation in response to treatment with mitochondrial  $\text{K}^+$  channel openers in cerebral arteries [30]. This effect can be inhibited by TMPyP.

Local activation of  $\text{Ca}^{2+}$  sparks close to sites of mitochondrial  $\Delta\Psi_m$  depolarization was first observed by Zorov et al [31] after laser-induced mitochondrial permeability transition pore activation. This study established the concept of mitochondrial ROS-induced ROS release, whereby a certain amount of oxidative stress leads to a regenerative burst of ROS

production as the mitochondria depolarize and uncouple. Similarly, we have reported that ROS-induced ROS release plays a role in the scaling of local  $\Delta\Psi_m$  depolarization to the entire mitochondrial network of mitochondria of the cardiomyocyte when a critical fraction of mitochondria reach a threshold level of oxidative stress [20], albeit through the activation of IMAC rather than the mPTP. Using a method similar to ours, another recent study also supported a link between mitochondrial ROS production and increased  $\text{Ca}^{2+}$  spark activity. In a study by Yan et al [32], laser-induced ROS production initiated a wave of oxidation of the ROS probe (CM-DCF) associated with an increase in  $\text{Ca}^{2+}$  spark frequency (measured using the  $\text{Ca}^{2+}$  indicator Rhod-2), first near the illumination site and later more widespread throughout the cell. The enhancement in  $\text{Ca}^{2+}$  spark frequency was prevented by treatment with either TMPyP or myxothiazol, which (as we have shown) inhibit mitochondrial ROS production and  $\Delta\Psi_m$  oscillations [15]. Although mitochondrial NADH or  $\Delta\Psi_m$  signals were not measured in that study, some cells showed oscillatory changes in ROS production with a mixed effect on spark frequency: early in the experiment spark frequency was enhanced, but later, spark frequency decreased when ROS production increased.

In the present work, we could directly correlate changes in  $\text{Ca}^{2+}$  spark frequency with indices of the mitochondrial energy and redox states ( $\Delta\Psi_m$ , NADH and GSH), enabling us to assess the roles of mitochondrial superoxide production, IMAC, mPTP, and the mitochondrial benzodiazepine receptor in the response. During whole-cell mitochondrial oscillations, we have shown that  $\Delta\Psi_m$  depolarizes and NADH oxidizes rapidly, with a concomitant burst of ROS production, which is then followed by a slower recovery phase with the cycle repeating approximately every 100 sec. Cellular GSH and  $\Delta\Psi_m$  oscillate in parallel, with the oxidation phase slightly preceding the rapid  $\Delta\Psi_m$  depolarization (Figure 4B). The present findings reveal that  $\text{Ca}^{2+}$  spark frequency increases by more than two-fold during each depolarization cycle and decreases to basal levels upon mitochondrial repolarization. The dynamic relationship between mitochondrial superoxide production,  $\text{Ca}^{2+}$  spark frequency and NADH oxidation was directly elucidated, confirming that high rates of mitochondrial ROS production correspond to increased  $\text{Ca}^{2+}$  spark frequency. We observed no significant change in  $\text{Ca}^{2+}$  spark amplitude or time-to-peak, nor the cytosolic  $\text{Ca}^{2+}$  during mitochondrial oscillations.

Suppression of both the mitochondrial oscillations and the effects on  $\text{Ca}^{2+}$  sparks by TMPyP indicates a common mechanism consistent with the ROS-dependent oscillator we have previously studied. Importantly, this was verified by observing that  $\text{Ca}^{2+}$  spark frequency declined in association with reduction of the NADH pool and  $\Delta\Psi_m$  stabilization in the presence of 4'-Cl-DZP. Furthermore, the oscillations in  $\Delta\Psi_m$  were not prevented by CsA, an inhibitor of the mPTP, although the peak  $\text{Ca}^{2+}$  spark rate during  $\Delta\Psi_m$  depolarization in CsA was less than the peak rate in the absence of CsA. The latter was unlikely to be due to mPTP opening contributing to the mitochondrial depolarization since CsA apparently impaired  $\Delta\Psi_m$  recovery during each cycle (cf Figure 6A). Rather, the CsA effect may be attributed to its effects on the RyR multiprotein complex ([33, 34]); nevertheless, all mitochondrial effects on  $\text{Ca}^{2+}$  spark frequency were still completely reversed by treatment with 4'-Cl-DZP after CsA washout.

Because loss of mitochondrial function will change a number of intracellular modulatory factors, and modify a number of ion transport proteins, further investigation will be required to assess the total effect of mitochondrial depolarization on the  $\text{Ca}^{2+}$  handling subsystem. As we have previously reported [15], sarcolemmal  $\text{K}_{\text{ATP}}$  channels are activated during the oscillations in  $\Delta\Psi_m$ , indicating that the ATP/ADP ratio decreases significantly, which would also increase free  $\text{Mg}^{2+}$ . These changes would tend to suppress the activity of the SR  $\text{Ca}^{2+}$  ATPase, the L-type  $\text{Ca}^{2+}$  channel, and the RyR, so it is not likely to account for the increased  $\text{Ca}^{2+}$  spark frequency. Numerous reports have revealed that cysteine oxidation

events can have important functional consequences for an array of signal transduction cascades, making apparent that multiple classes of regulatory proteins are reversibly oxidized by  $\text{H}_2\text{O}_2$  among other oxidants [35]. The increase in resting  $\text{Ca}^{2+}$  spark activity described herein is consistent with the effects of thiol oxidation on RyR, consistent with our earlier studies showing that oxidation of the glutathione pool occurs during the metabolic oscillations [16], but the precise modulator of the SR  $\text{Ca}^{2+}$  release channel is difficult to select from among several candidates. The most straightforward interpretation would be that oxidation of the redox pool (including GSH and NADH), depleted during the sequential reactions of superoxide dismutase and glutathione peroxidase and supported by the oxidation of NADPH, directly modifies reactive cysteines on the cytoplasmic face of the RyR. However, we cannot exclude direct effects of individual reactive molecules on channel open probability: for example,  $\text{H}_2\text{O}_2$  (and hydroxyl radicals) [36], NO [37], nitroxyl [38] and  $\text{NAD}^+$  [39] have been shown to increase RyR activity in channel reconstitution experiments, and the skeletal RyR reportedly contains an oxidoreductase-homology domain with an  $\text{NAD}^+$  binding site [40]. With respect to a possible direct effect of superoxide on RyR, Zima et al [39] reported that superoxide suppressed  $\text{Ca}^{2+}$  spark activity when generated by the xanthine/xanthine oxidase reaction, yet one must also consider that superoxide plays a central role in the autocatalytic feedback mechanism of the mitochondrial oscillator [15, 41] and thus will alter the levels and redox status of all other factors.

Although covalent modifications of RyR, including S-glutathionylation [42] and S-nitrosylation [43], are known to modify channel gating properties, these processes would have to be very quickly reversed (within seconds) to account for the phasic changes in  $\text{Ca}^{2+}$  spark frequency described here: this may be possible based on current paradigms[44]. Another interesting alternative could be that the RyR open probability is responding to oxidation of the channel from the luminal side of the SR, as suggested by several studies[45–47]. At present, we have no information about how the changes in mitochondrial energy state might affect intraluminal redox potential, which is thought to be much more oxidized than the cytoplasm [48], however,  $\text{H}_2\text{O}_2$  readily diffuses through membranes and the SR surrounds, and is in direct contact with the mitochondrial outer membrane.

## 5. Conclusions

We conclude that during oxidative stress, the amplifying effect of mitochondrial RIRR to activate IMAC not only evokes oscillations in the energy state to influence sarcolemmal KATP currents, but also modulates the  $\text{Ca}^{2+}$  handling system directly by governing the local redox environment near the dyad. During acute  $\Delta\Psi_m$  depolarization, mitochondria elicit oxidation of the redox environment, favoring modification of critical thiol groups on the RyR receptor, increasing its open probability independent of changes in SR  $\text{Ca}^{2+}$  load in the short term. The results demonstrate that there is a dynamic mechanistic link between mitochondrial polarization state and resting  $\text{Ca}^{2+}$  spark rate. Defining all of the metabolic factors affecting  $\text{Ca}^{2+}$  release in beating cells will, however, require further investigation.

### Research highlights

- The present study examines how mitochondrial energy state dynamically modulates spontaneous  $\text{Ca}^{2+}$  release in ventricular cardiomyocytes
- Simultaneous measurements of mitochondrial inner membrane potential ( $\Delta\Psi_m$ ), reactive oxygen species (ROS), and  $\text{Ca}^{2+}$  sparks revealed that during  $\Delta\Psi_m$  and redox oscillations induced by oxidative stress, the resting  $\text{Ca}^{2+}$  spark rate is inversely correlated with the energy state of mitochondria, i.e., when the mitochondrial network depolarizes, spark rate increases and when it repolarizes, spark rate decreases

- The regulatory mechanism involves changes in the local oxidative environment occurring during mitochondrial ROS-induced release as a consequence of redox-sensitive alterations in SR Ca<sup>2+</sup> release channel activity.

## Supplementary Material

Refer to Web version on PubMed Central for supplementary material.

## Acknowledgments

This study was supported by NIH grants R33-HL87345, R37-HL54598 and R01-HL101235 (to B.O'R.) and K99-HL095648 (to L.Z.).

## REFERENCES

1. Maack C, O'Rourke B. Excitation-contraction coupling and mitochondrial energetics. Basic research in cardiology. 2007 Sep; 102(5):369–392. [PubMed: 17657400]
2. Territo PR, French SA, Dunleavy MC, Evans FJ, Balaban RS. Calcium activation of heart mitochondrial oxidative phosphorylation: rapid kinetics of mVO<sub>2</sub>, NADH, AND light scattering. The Journal of biological chemistry. 2001 Jan 26; 276(4):2586–2599. [PubMed: 11029457]
3. Maack C, Cortassa S, Aon MA, Ganesan AN, Liu T, O'Rourke B. Elevated cytosolic Na<sup>+</sup> decreases mitochondrial Ca<sup>2+</sup> uptake during excitation-contraction coupling and impairs energetic adaptation in cardiac myocytes. Circulation research. 2006 Jul 21; 99(2):172–182. [PubMed: 16778127]
4. Dedkova EN, Blatter LA. Mitochondrial Ca<sup>2+</sup> and the heart. Cell calcium. 2008 Jul; 44(1):77–91. [PubMed: 18178248]
5. Shannon TR, Bers DM. Assessment of intra-SR free [Ca] and buffering in rat heart. Biophysical journal. 1997 Sep; 73(3):1524–1531. [PubMed: 9284319]
6. Noma A, Shibasaki T. Membrane current through adenosine-triphosphate-regulated potassium channels in guinea-pig ventricular cells. The Journal of physiology. 1985 Jun.363:463–480. [PubMed: 2410609]
7. O'Rourke B, Backx PH, Marban E. Phosphorylation-independent modulation of L-type calcium channels by magnesium-nucleotide complexes. Science. 1992; 257(5067):245–248. [PubMed: 1321495]
8. Hilgemann DW. Regulation and deregulation of cardiac Na<sup>(+)</sup>-Ca<sup>2+</sup> exchange in giant excised sarcolemmal membrane patches. Nature. 1990 Mar 15; 344(6263):242–245. [PubMed: 2314460]
9. Meissner G, Henderson JS. Rapid calcium release from cardiac sarcoplasmic reticulum vesicles is dependent on Ca<sup>2+</sup> and is modulated by Mg<sup>2+</sup>, adenine nucleotide, and calmodulin. The Journal of biological chemistry. 1987 Mar 5; 262(7):3065–3073. [PubMed: 2434495]
10. Kowaltowski AJ, de Souza-Pinto NC, Castilho RF, Vercesi AE. Mitochondria and reactive oxygen species. Free Radic Biol Med. 2009 Aug 15; 47(4):333–343. [PubMed: 19427899]
11. Stowe DF, Camara AK. Mitochondrial reactive oxygen species production in excitable cells: modulators of mitochondrial and cell function. Antioxidants & redox signaling. 2009 Jun; 11(6): 1373–1414. [PubMed: 19187004]
12. Murphy MP. How mitochondria produce reactive oxygen species. Biochem J. 2009 Jan 1; 417(1): 1–13. [PubMed: 19061483]
13. Aon MA, Cortassa S, O'Rourke B. Redox-optimized ROS balance: A unifying hypothesis. Biochimica et biophysica acta. 2010 June – July; 1797(6–7):865–877. [PubMed: 20175987]
14. Aon MA, Cortassa S, Maack C, O'Rourke B. Sequential opening of mitochondrial ion channels as a function of glutathione redox thiol status. The Journal of biological chemistry. 2007 Jul 27; 282(30):21889–21900. [PubMed: 17540766]
15. Aon MA, Cortassa S, Marban E, O'Rourke B. Synchronized whole cell oscillations in mitochondrial metabolism triggered by a local release of reactive oxygen species in cardiac

- myocytes. *The Journal of biological chemistry*. 2003 Nov 7; 278(45):44735–44744. [PubMed: 12930841]
16. Cortassa S, Aon MA, Winslow RL, O'Rourke B. A mitochondrial oscillator dependent on reactive oxygen species. *Biophysical journal*. 2004 Sep; 87(3):2060–2073. [PubMed: 15345581]
  17. Xia R, Stangler T, Abramson JJ. Skeletal muscle ryanodine receptor is a redox sensor with a well defined redox potential that is sensitive to channel modulators. *The Journal of biological chemistry*. 2000 Nov 24; 275(47):36556–36561. [PubMed: 10952995]
  18. O'Rourke B, Ramza BM, Marban E. Oscillations of membrane current and excitability driven by metabolic oscillations in heart cells. *Science*. 1994; 265(5174):962–966. [PubMed: 8052856]
  19. Picht E, Zima AV, Blatter LA, Bers DM. SparkMaster: automated calcium spark analysis with ImageJ. *American journal of physiology*. 2007 Sep; 293(3):C1073–C1081. [PubMed: 17376815]
  20. Aon MA, Cortassa S, O'Rourke B. Percolation and criticality in a mitochondrial network. *Proceedings of the National Academy of Sciences of the United States of America*. 2004 Mar 30; 101(13):4447–4452. [PubMed: 15070738]
  21. Kinnally KW, Antonenko YN, Zorov DB. Modulation of inner mitochondrial membrane channel activity. *Journal of bioenergetics and biomembranes*. 1992 Feb; 24(1):99–110. [PubMed: 1380510]
  22. Akar FG, Aon MA, Tomaselli GF, O'Rourke B. The mitochondrial origin of postischemic arrhythmias. *J Clin Invest*. 2005 Dec; 115(12):3527–3535. [PubMed: 16284648]
  23. Anzai K, Ogawa K, Ozawa T, Yamamoto H. Oxidative modification of ion channel activity of ryanodine receptor. *Antioxidants & redox signaling*. 2000 Spring; 2(1):35–40. [PubMed: 11232597]
  24. Dulhunty A, Haarmann C, Green D, Hart J. How many cysteine residues regulate ryanodine receptor channel activity? *Antioxidants & redox signaling*. 2000 Spring; 2(1):27–34. [PubMed: 11232596]
  25. Hamilton SL, Reid MB. RyR1 modulation by oxidation and calmodulin. *Antioxidants & redox signaling*. 2000 Spring; 2(1):41–45. [PubMed: 11232598]
  26. Meissner G. Molecular regulation of cardiac ryanodine receptor ion channel. *Cell calcium*. 2004 Jun; 35(6):621–628. [PubMed: 15110152]
  27. Salama G, Menshikova EV, Abramson JJ. Molecular interaction between nitric oxide and ryanodine receptors of skeletal and cardiac sarcoplasmic reticulum. *Antioxidants & redox signaling*. 2000 Spring; 2(1):5–16. [PubMed: 11232600]
  28. Liu G, Abramson JJ, Zable AC, Pessah IN. Direct evidence for the existence and functional role of hyperreactive sulfhydryls on the ryanodine receptor-triadin complex selectively labeled by the coumarin maleimide 7-diethylamino-3-(4'-maleimidylphenyl)-4-methylcoumarin. *Molecular pharmacology*. 1994 Feb; 45(2):189–200. [PubMed: 8114670]
  29. Isaeva EV, Shkryl VM, Shirokova N. Mitochondrial redox state and Ca<sup>2+</sup> sparks in permeabilized mammalian skeletal muscle. *The Journal of physiology*. 2005 Jun 15; 565(Pt 3):855–872. [PubMed: 15845582]
  30. Xi Q, Cheranov SY, Jaggar JH. Mitochondria-derived reactive oxygen species dilate cerebral arteries by activating Ca<sup>2+</sup> sparks. *Circulation research*. 2005 Aug 19; 97(4):354–362. [PubMed: 16020754]
  31. Zorov DB, Filburn CR, Klotz LO, Zweier JL, Sollott SJ. Reactive oxygen species (ROS)-induced ROS release: a new phenomenon accompanying induction of the mitochondrial permeability transition in cardiac myocytes. *The Journal of experimental medicine*. 2000 Oct 2; 192(7):1001–1014. [PubMed: 11015441]
  32. Yan Y, Liu J, Wei C, Li K, Xie W, Wang Y, et al. Bidirectional regulation of Ca<sup>2+</sup> sparks by mitochondria-derived reactive oxygen species in cardiac myocytes. *Cardiovascular research*. 2008 Jan 15; 77(2):432–441. [PubMed: 18006452]
  33. Bandyopadhyay A, Shin DW, Ahn JO, Kim DH. Calcineurin regulates ryanodine receptor/Ca<sup>2+</sup>-release channels in rat heart. *Biochem J*. 2000 Nov 15; 352(Pt 1):61–70. [PubMed: 11062058]
  34. Park KS, Kim TK, Kim DH. Cyclosporin A treatment alters characteristics of Ca<sup>2+</sup>-release channel in cardiac sarcoplasmic reticulum. *The American journal of physiology*. 1999 Mar; 276(3 Pt 2):H865–H872. [PubMed: 10070069]

35. Janssen-Heininger YM, Mossman BT, Heintz NH, Forman HJ, Kalyanaraman B, Finkel T, et al. Redox-based regulation of signal transduction: principles, pitfalls, and promises. *Free Radic Biol Med*. 2008 Jul 1; 45(1):1–17. [PubMed: 18423411]
36. Anzai K, Ogawa K, Kuniyasu A, Ozawa T, Yamamoto H, Nakayama H. Effects of hydroxyl radical and sulfhydryl reagents on the open probability of the purified cardiac ryanodine receptor channel incorporated into planar lipid bilayers. *Biochemical and biophysical research communications*. 1998 Aug 28; 249(3):938–942. [PubMed: 9731240]
37. Phimister AJ, Lango J, Lee EH, Ernst-Russell MA, Takeshima H, Ma J, et al. Conformation-dependent stability of junctophilin 1 (JP1) and ryanodine receptor type 1 (RyR1) channel complex is mediated by their hyper-reactive thiols. *The Journal of biological chemistry*. 2007 Mar 23; 282(12):8667–8677. [PubMed: 17237236]
38. Tocchetti CG, Wang W, Froehlich JP, Huke S, Aon MA, Wilson GM, et al. Nitroxyl improves cellular heart function by directly enhancing cardiac sarcoplasmic reticulum Ca<sup>2+</sup> cycling. *Circulation research*. 2007 Jan 5; 100(1):96–104. [PubMed: 17138943]
39. Zima AV, Copello JA, Blatter LA. Effects of cytosolic NADH/NAD(+) levels on sarcoplasmic reticulum Ca(2+) release in permeabilized rat ventricular myocytes. *The Journal of physiology*. 2004 Mar 16; 555(Pt 3):727–741. [PubMed: 14724208]
40. Baker ML, Serysheva II, Sencer S, Wu Y, Ludtke SJ, Jiang W, et al. The skeletal muscle Ca<sup>2+</sup> release channel has an oxidoreductase-like domain. *Proceedings of the National Academy of Sciences of the United States of America*. 2002 Sep 17; 99(19):12155–12160. [PubMed: 12218169]
41. Zhou L, Aon MA, Almas T, Cortassa S, Winslow RL, O'Rourke B. A reaction-diffusion model of ROS-induced ROS release in a mitochondrial network. *PLoS Comput Biol*. 2010; 6(1):e1000657. [PubMed: 20126535]
42. Hidalgo C, Sanchez G, Barrientos G, Aracena-Parks P. A transverse tubule NADPH oxidase activity stimulates calcium release from isolated triads via ryanodine receptor type 1 S-glutathionylation. *The Journal of biological chemistry*. 2006 Sep 8; 281(36):26473–26482. [PubMed: 16762927]
43. Aracena P, Tang W, Hamilton SL, Hidalgo C. Effects of S-glutathionylation and S-nitrosylation on calmodulin binding to triads and FKBP12 binding to type 1 calcium release channels. *Antioxidants & redox signaling*. 2005 Jul–Aug; 7(7–8):870–881. [PubMed: 15998242]
44. Hess DT, Matsumoto A, Kim SO, Marshall HE, Stamler JS. Protein S-nitrosylation: purview and parameters. *Nature reviews*. 2005 Feb; 6(2):150–166.
45. Oba T, Ishikawa T, Yamaguchi M. Sulfhydryls associated with H<sub>2</sub>O<sub>2</sub>-induced channel activation are on luminal side of ryanodine receptors. *The American journal of physiology*. 1998 Apr; 274(4 Pt 1):C914–C921. [PubMed: 9575787]
46. Wei L, Abdellatif YA, Liu D, Kimura T, Coggan M, Gallant EM, et al. Muscle-specific GSTM2-2 on the luminal side of the sarcoplasmic reticulum modifies RyR ion channel activity. *The international journal of biochemistry & cell biology*. 2008; 40(8):1616–1628.
47. Feng W, Liu G, Allen PD, Pessah IN. Transmembrane redox sensor of ryanodine receptor complex. *The Journal of biological chemistry*. 2000 Nov 17; 275(46):35902–35907. [PubMed: 10998414]
48. Hwang C, Sinsky AJ, Lodish HF. Oxidized redox state of glutathione in the endoplasmic reticulum. *Science*. 1992 Sep 11; 257(5076):1496–1502. [PubMed: 1523409]

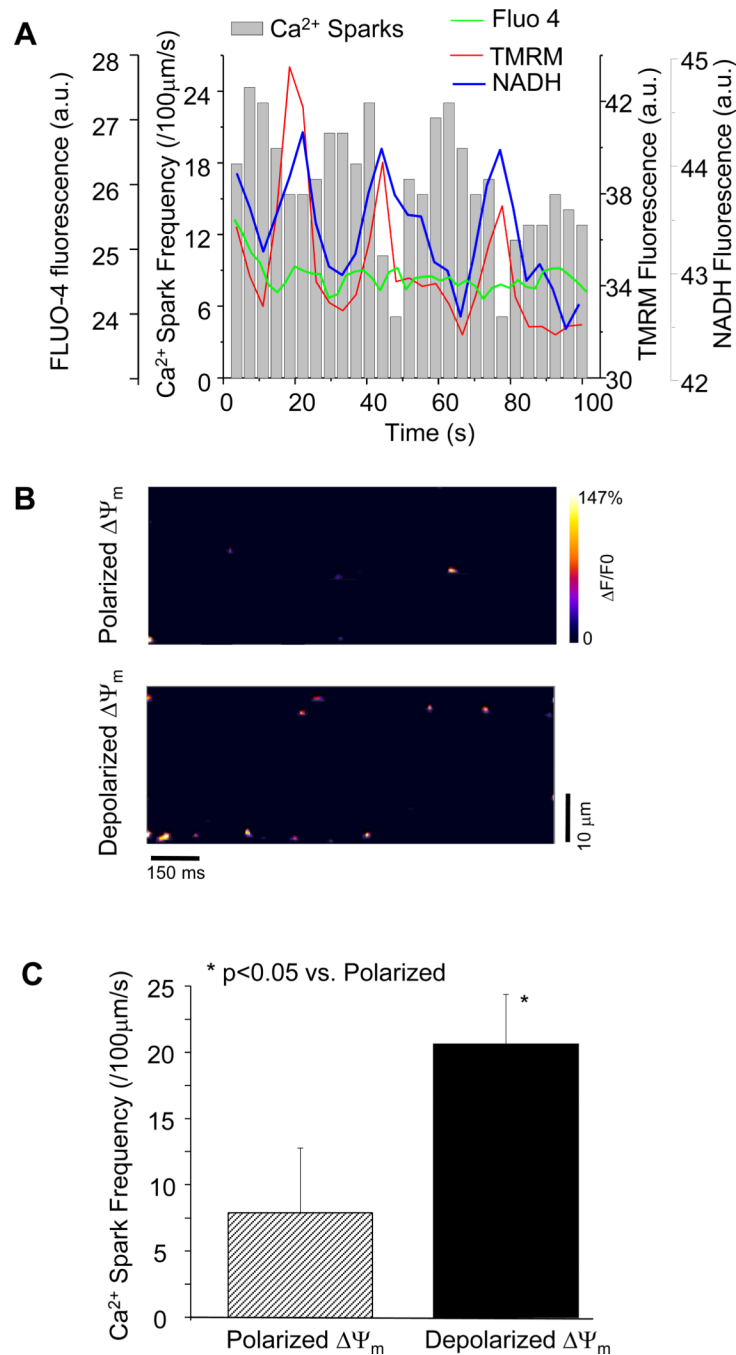


**Figure 1.**

Influence of oxidative stress on mitochondrial  $\Delta\Psi_m$  and Ca<sup>2+</sup> spark frequency. (A) Phase relationship among oscillations in  $\Delta\Psi_m$ , NADH, and cyclic changes of Ca<sup>2+</sup> sparks as a result of oxidative stress induced by a localized laser flash (a.u.: arbitrary units of fluorescence). The green line indicates Fluo-4 fluorescence intensity that reflects average cytosolic Ca<sup>2+</sup>; (B) Representative contour plots showing increased Ca<sup>2+</sup> spark frequency when mitochondria depolarized; and (C) Quantitative comparison of Ca<sup>2+</sup> spark frequency between  $\Delta\Psi_m$  polarization and depolarization states.

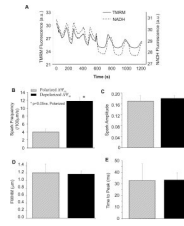


**Figure 2.** Analysis of  $\text{Ca}^{2+}$  spark properties. (A) Oscillations in  $\Delta\Psi_m$  and NADH triggered by repeating laser line scanning; (B) Influence of  $\Delta\Psi_m$  energy state on  $\text{Ca}^{2+}$  spark frequency; and (C–E) Modulation of frequency, but not amplitude, FWHM, or time-to-peak of  $\text{Ca}^{2+}$  sparks by mitochondrial energy state.

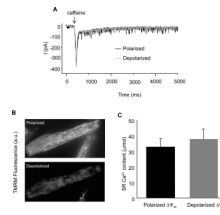


**Figure 3.** SR Ca<sup>2+</sup> loading and mitochondrial energetic states. (A) Representative sarcolemmal NCX current recorded before and after UV light induced mitochondrial membrane potential depolarization; and (B) Comparison of SR Ca<sup>2+</sup> content before and after mitochondrial membrane potential depolarization.

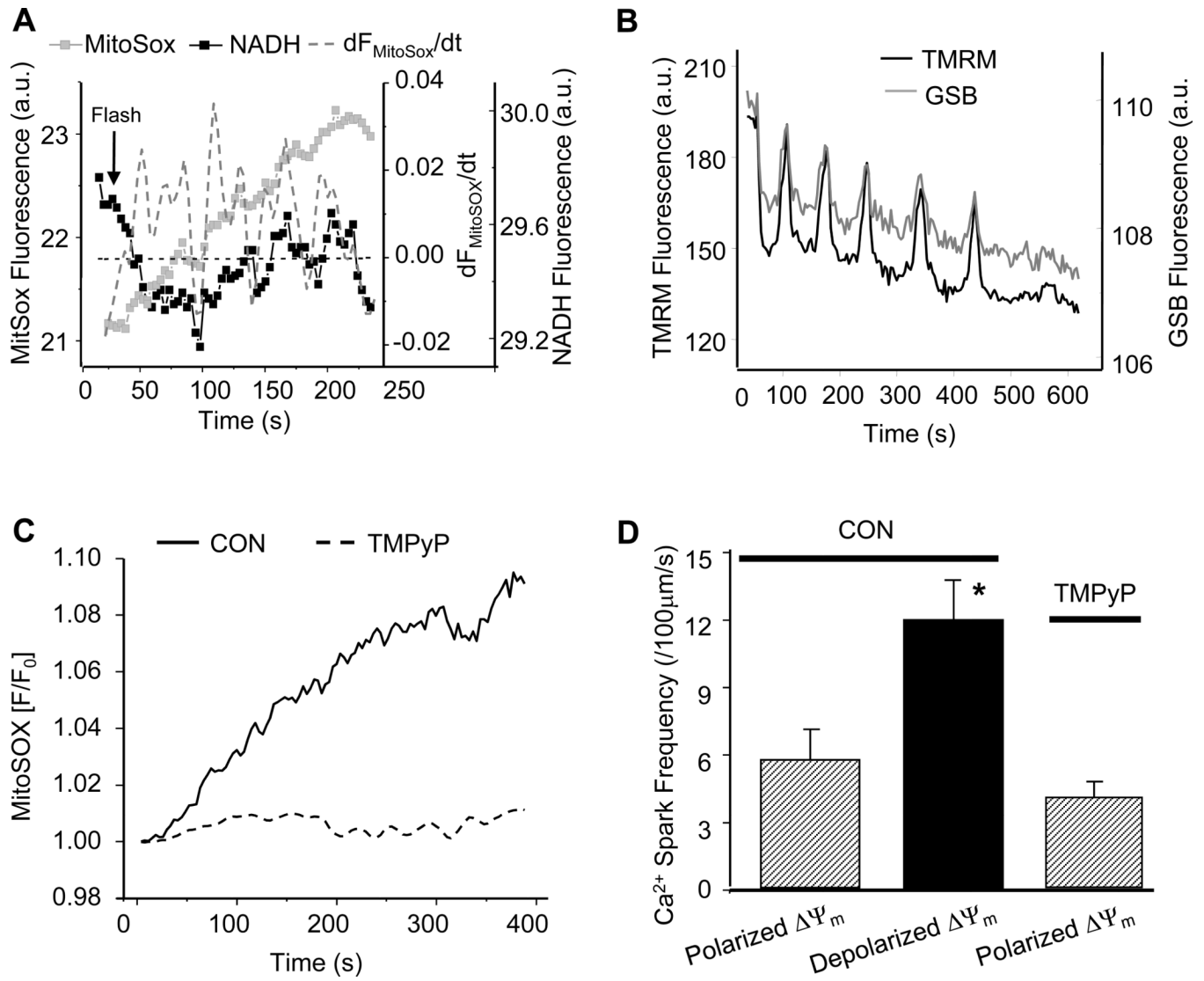


**Figure 4.** Suppression of  $\Delta\Psi_m$  oscillations and enhanced  $\text{Ca}^{2+}$  spark frequency by the superoxide scavenger TMPyP. (A) Dynamics of the rate of  $\text{O}_2^{\cdot-}$  production (MitoSOX) and NADH fluorescence during mitochondrial oscillations (TMRM was not loaded in this experiment due to overlap with the MitoSOX emission); (B) Dynamic changes of  $\Delta\Psi_m$  and GSH during mitochondrial oscillations; (C) Effect of TMPyP on ROS production; and (D) Effect of  $\text{O}_2^{\cdot-}$  scavenger on  $\text{Ca}^{2+}$  spark frequency.

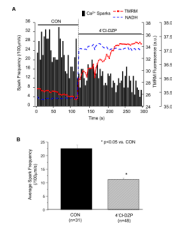


**Figure 5.**

Effect of the mitochondrial benzodiazepine receptor ligand 4'Cl-DZP on the occurrence of Ca<sup>2+</sup> sparks in the presence of oxidative stress. (A) Immediate increase of NADH, recovery of membrane potential, and suppression of Ca<sup>2+</sup> sparks after addition of 4'Cl-DZP; and (B) Comparison of average Ca<sup>2+</sup> spark frequency before and after the addition of 4'Cl-DZP.

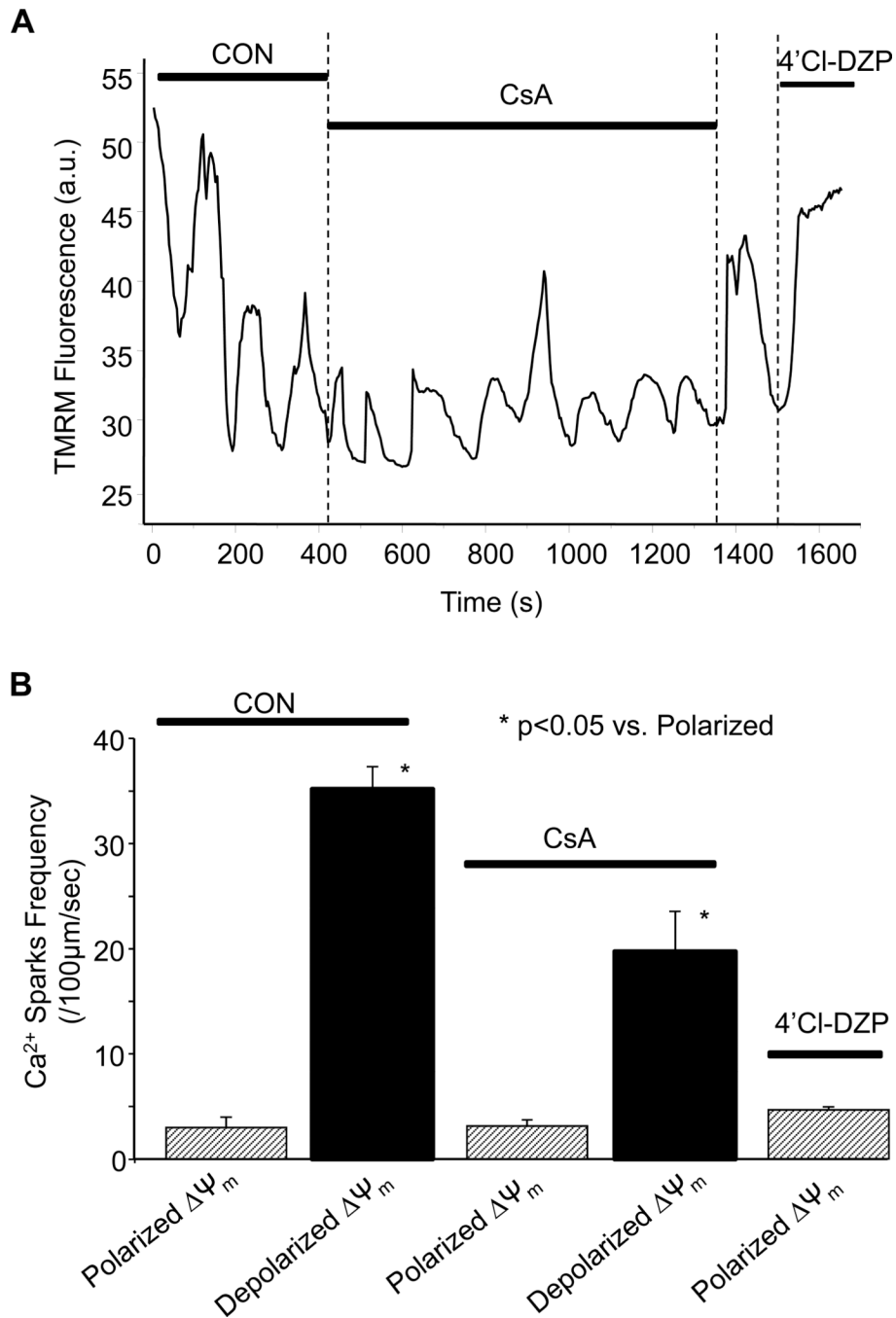


**Figure 6.** Effect of mitochondrial permeability transition pore (mPTP) blocker cyclosporine A (CsA) on the occurrence of Ca<sup>2+</sup> sparks during mitochondrial  $\Delta\Psi_m$  oscillation. (A) Effect of acute addition of CsA on  $\Delta\Psi_m$  oscillations and Ca<sup>2+</sup> spark frequency; and (B) Summary of Ca<sup>2+</sup> spark frequency as a function of  $\Delta\Psi_m$  during control (CON), after adding CsA or in the presence of 4'Cl-DZP after CsA washout.